Molecular hyperfine fields in organic magnetoresistance devices

Ronaldo Giro,[1,*] Flávia P. Rosselli,[1] Rafael dos Santos Carvalho,[2] Rodrigo B. Capaz,[1,3]
Marco Cremona,[1,2] and Carlos A. Achete[1,4]

[1]*Divisão de Metrologia de Materiais, Instituto Nacional de Metrologia, Qualidade e Tecnologia (INMETRO), CEP 25250-020, Duque de Caxias-RJ, Brazil*

[2]*LOEM, Departamento de Física, Pontifícia Universidade Católica do Rio de Janeiro, PUC-Rio, CP 38071, CEP 22453-970, Rio de Janeiro-RJ, Brazil*

[3]*Instituto de Física, Universidade Federal do Rio de Janeiro, Caixa Postal 68528, Brazil*

[4]*Departamento de Engenheria Metalúrgica e de Materiais, Universidade Federal do Rio de Janeiro, CP 68505, CEP 21945-970, Rio de Janeiro-RJ, Brazil*

(Received 13 August 2012; published 22 March 2013)

We calculate molecular hyperfine fields in organic magnetoresistance (OMAR) devices using *ab initio* calculations. To do so, we establish a protocol for the accurate determination of the average hyperfine field $B_{\rm hf}$ and apply it to selected molecular ions: NPB, TPD, and Alq_3. Then, we make devices with precisely the same molecules and perform measurements of the OMAR effect, in order to address the role of hole-transport layer in the characteristic magnetic field B_0 of OMAR. Contrary to common belief, we find that molecular hyperfine fields are not only caused by hydrogen nuclei. We also find that dipolar contributions to the hyperfine fields can be comparable to the Fermi contact contributions. However, such contributions are restricted to nuclei located in the same molecular ion as the charge carrier (intramolecular), as extramolecular contributions are negligible.

DOI: 10.1103/PhysRevB.87.125204 PACS number(s): 73.50.Jt, 31.30.Gs, 72.20.My, 81.05.Fb

The recent discovery of a large magnetoresistive effect (up to 10% at 10 mT and 300 K)[1] in organic light-emitting diodes (OLEDs), named organic magnetoresistance (OMAR), has called the attention of several research groups to a new area of study. In addition to its potential applications, OMAR poses a significant scientific puzzle since it is the only known example of large room-temperature magnetoresistance in nonmagnetic materials, with the exception of narrow-gap high-mobility materials, as reported by Sheng *et al.*[2] In order to explain this effect, several models have been proposed, sometimes with contradictory results.[3–8]

Although a definitive model to explain OMAR is apparently far from being established, the research performed so far in this area suggests that molecular hyperfine fields contribute to the OMAR effect.[2,5,8–10] However, there are contradictory results regarding the extension of this contribution. For instance, Rolfe *et al.*[11] constructed OLEDs based on fully deutered Alq_3, where the OMAR was expected to be significantly altered due to the increase of hyperfine interaction, caused by the larger nuclear spin of deuteron as compared to proton. They found no consistent differences between the deuterated and protiated devices, in magnitude or line shape of OMAR, for magnetic fields up to 300 mT. A similar study by Nguyen *et al.*[9] compared the magnetoelectroluminescente (MEL) of protiated and partially deuterated poly(dioctyloxy)phenylenevinylene based OLEDs, and they found that the saturation fields of the magnetic field effects on the MEL were reduced by a factor $\approx$2 in the deuterated material. They concluded that the hyperfine interaction is the main cause of MEL in OLEDs, and it is crucial to the other magnetic field effects. In a recent work, Rolfe *et al.*[8] proposed the separation of OMAR mechanism into three spin interaction processes, and argued that one of these processes, the intersystem crossing between polaron pairs, is strongly affected by deuteration. They suggested that only $\approx$30% of the total OMAR is influenced by deuteration (hyperfine interactions).

If OMAR is related to hyperfine interactions, it has been argued by many authors that the characteristic magnetic field B_0 of the OMAR effect, which follows empirical laws given by either non-Lorentzian $\Delta I(B)/I \propto B^2/(|B| + B_0)^2$ or Lorentzian $\Delta I(B)/I \propto B^2/(B^2 + B_0^2)$ line shapes, should be proportional to the average molecular hyperfine field $B_{\rm hf}$ felt by an electron or hole during the residence time of the hopping transport process.[2,5,10,12] Most currently available models suggest $B_0 = \alpha B_{\rm hf}$, with $\alpha \lesssim 3$.

Therefore, a complete and quantitative theory of the effect would have to address and solve three problems. (1) The accurate calculation of hyperfine tensors for each nuclei in OMAR molecules, obtained via a realistic description of electron or hole spin densities. (2) The proper definition and computation of the average molecular hyperfine field $B_{\rm hf}$. (3) A model to relate $B_{\rm hf}$ to the typical OMAR field B_0, preferably with the ability to describe and predict the B_0 dependence on several quantities such as temperature, layer thickness, and bias. Moreover, the model would have to be able to predict the line shape (Lorentzian or non-Lorentzian) of the observed OMAR. As we shall see, this work aims at solving problems (1) and (2). In addition, by combining theory and experiment, we address the role of hole-transport layer (HTL) in OMAR. As a consequence of our findings, we draw important conclusions regarding the role played by hyperfine interactions in OMAR.

The effective molecular hyperfine field B_{hf}. The hyperfine interaction Hamiltonian between an electron-spin distribution (localized within a single molecule) and a single nuclear spin i is

$$H_i = \mathbf{S}_e \mathbf{A}^i \mathbf{I}^i, \tag{1}$$

where $\mathbf{S}_e$ is the electron spin, $\mathbf{I}^i$ is the nuclear spin, and $\mathbf{A}^i$ is the hyperfine tensor for atom i. The components of the $\mathbf{A}^i$

TABLE I. Properties of isotopes with nonzero spin. S_e and I^i are the electron and nuclear spin quantum numbers; p_i is the natural abundance of isotope i. Spin units in $\hbar$. Magnetic moments μ_e and μ_I^i are in units of the nuclear magneton $\mu_N = 5.050787 \times 10^{-27}$ J/T. The natural abundance is taken from Ref. 14, and the magnetic moments from Refs. 15 and 16.

Nucleus (i)	p_i	$I^i[\hbar]$	$S_e[\hbar]$	$\mu_I^i[\mu_N]$	$\mu_e[\mu_N]$
e			1/2		1838.28
^{1}H	99.9885%	1/2		2.79284	
^{13}C	1.07%	1/2		0.702411	
^{14}N	99.632%	1		0.4037607	
^{17}O	0.038%	5/2		−1.89380	
^{27}Al	100%	5/2		3.641504	

tensor are given by[13]

$$A^i_{mn} = \frac{\mu_e \mu_I^i}{S_e I^i}\left[\frac{2\mu_0}{3}\delta_{mn}\int dr\, \delta_T(\mathbf{r}) n_s(\mathbf{r}) + \frac{\mu_0}{4\pi}\int d^3r \frac{n_s(\mathbf{r})}{r^3}\left(\frac{3r_m r_n - \delta_{mn}\mathbf{r}^2}{r^2}\right)\right], \quad (2)$$

where S_e and I^i are the electron and nuclear spin quantum numbers, respectively (see Table I for details); μ_e is the electronic magnetic moment: $\mu_e \approx \mu_B = 9.274 \times 10^{-24}$ J/T (Bohr magneton); μ_I^i is the nuclear magnetic moment for nucleus i (see Table I); $n_s(\mathbf{r})$ is the electronic spin density: $n_s(\mathbf{r}) = n_\uparrow(\mathbf{r}) - n_\downarrow(\mathbf{r})$; δ_T is a smeared-out δ function as described in Ref. 13; and $\mathbf{r}$ is the electron position measured from the nucleus i. The first term in Eq. (2) is the isotropic Fermi contact term and the second term is the anisotropic dipole term, so we can decompose the tensor $\mathbf{A}^i$ as

$$\mathbf{A}^i = A^i_{\rm iso}\mathbf{1} + \mathbf{A}^i_{\rm dip}. \quad (3)$$

It is convenient to express the A^i_{mn} components in magnetic field units:

$$A^i_{mn} \leftarrow \frac{\hbar^2}{g_e \mu_B} A^i_{mn}. \quad (4)$$

Then, using Eq. (1), we define the total hyperfine magnetic field from all the nuclei in a single molecule acting on the electron spin as

$$\mathbf{B}_{\rm hf} = \sum_i \mathbf{A}^i \frac{\mathbf{I}^i}{\hbar}. \quad (5)$$

Notice that the sum runs over all nuclear spins in the organic layer: those located at the same molecule where the extra electron or hole is (intramolecular contributions) and those located in neighboring molecules (extramolecular contributions). Also notice that, at this point, this definition is of limited practical use, since the nuclear spins $\mathbf{I}^i$ are spin operators and not vectors. To define an effective magnetic vector field acting on the electron, we generalize the semiclassical description of Schulten and Wolynes[17] and treat the nuclear spins $\mathbf{I}^i$ as classical vectors of magnitude $p_i\sqrt{I^i(I^i+1)}$ and random orientations, where p_i is the natural abundance of the isotope with nonzero nuclear spin (see Table I). Then, the sum expressed in Eq. (5) can be performed and the effective hyperfine field is calculated as

$$B_{\rm hf} = \langle|\mathbf{B}_{\rm hf}|\rangle, \quad (6)$$

where the average is taken over many realizations of the orientations of the random vectors $\mathbf{I}^i$. Following this protocol, it is also possible to extract the contributions of the Fermi contact and dipolar term [see Eq. (3)] and of different chemical elements to $B_{\rm hf}$. We can also separate the intramolecular and extramolecular contributions. This will allow us to test a widespread assumption from previous works: that the hyperfine field is mainly due to the Fermi contact term of hydrogen nuclei.[2,5,6,10,17,18]

In OMAR devices, the transport mechanism consists of molecular hopping of electrons and holes. The unpaired charge carrier will be responsible for the spin density that will in turn couple to the nuclear spins through the hyperfine interaction. Therefore, we simulate the molecules with one added or removed electron (anion or cation). To ensure that our approach has quantitative and predictive capabilities, the molecular geometry and spin density must be calculated using *ab initio* methods. We use the Gaussian03 program[19] within density functional theory. For the exchange-correlation term, the hybrid functional PBE1PBE is used.[20–22] For the expansion of wave functions, the 6-31G(d,p)[23] basis set is employed.[24] The geometry of cation and anion molecules are optimized in vacuum.[25] Once the geometric parameters are optimized, the hyperfine parameters are calculated with the gauge invariant atomic orbitals method. To calculate extramolecular contributions to the hyperfine field,[26] we use atomic positions corresponding to the crystalline packing obtained from x-ray measurements.[27–29]

For reasons that will become clear below, we analyze three different organic molecules (see Fig. 1): N,N'-diphenyl-N,N'-bis(1-napthyl)-1,1'-biphenyl-4,4'-diamine (β-NPB), triphenyl-diamine derivative,N,N'-diphenyl-N,N'bis(3-methylphenyl)-(1,1'-biphenyl)-4,4'diamine (TPD), and mer-Tris(8-hydroxyquinolato)aluminum (Alq_3). TPD and NPB are commonly used as hole-transport materials and Alq3 serves both as electron-transport and light-emitting material in organic light-emitting devices (OLEDs). Table II shows our results for $B_{\rm hf}$ and its components $B_{\rm iso}$ (Fermi contact), $B_{\rm dip}$ (total dipolar contribution), and $B^{\rm intra}_{\rm dip}$ (intramolecular dipolar contribution) for the three molecular ions (cation and anion in each case) and contributions from the relevant chemical

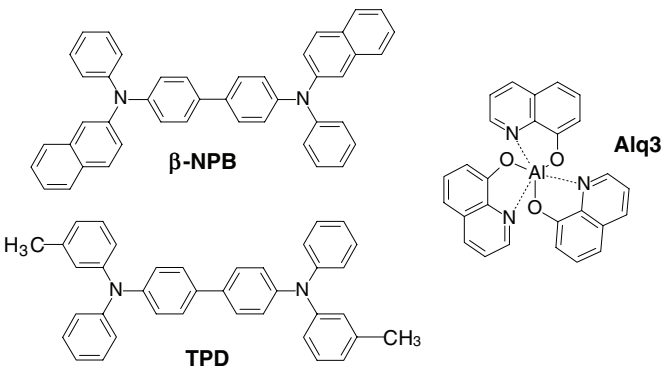

FIG. 1. Two-dimensional schematic representation of molecules considered in this work.

TABLE II. Effective molecular magnetic field B_{hf} from hyperfine interactions for Alq_3, NPB, and TPD ions and contributions of Fermi contact, total dipolar and intramolecular dipolar terms, as well of different chemical species. Units of B_{hf} and its components are mT. Note that the different contributions do not add up to the total values because they represent the sum over vectors with random orientations, as described in the text.

	Cation				Anion			
Molecule	B_{hf}	B_{iso}	B_{dip}	B_{dip}^{intra}	B_{hf}	B_{iso}	B_{dip}	B_{dip}^{intra}
Alq_3								
Hydrogen	1.10	1.00	0.41	0.39	1.17	1.02	0.44	0.42
Nitrogen	0.09	0.08	0.03	0.03	0.62	0.49	0.49	0.49
Aluminum	0.80	0.80	0.04	0.03	0.44	0.41	0.10	0.04
Total	1.32	1.25	0.42	0.39	1.39	1.18	0.66	0.64
NPB								
Hydrogen	0.48	0.42	0.22	0.18	0.63	0.58	0.27	0.22
Nitrogen	1.29	0.83	0.88	0.87	0.19	0.17	0.04	0.04
Total	1.39	0.94	0.91	0.89	0.65	0.61	0.27	0.23
TPD								
Hydrogen	0.47	0.40	0.23	0.19	0.55	0.52	0.26	0.22
Nitrogen	1.31	0.84	0.90	0.89	0.28	0.27	0.03	0.03
Total	1.40	0.93	0.93	0.91	0.61	0.58	0.26	0.23

species. We first note that the magnitude of B_{hf} is very similar for Alq_3 anion and NPB and TPD cations (1.32 mT, 1.39 mT, and 1.40 mT, respectively). This is an important condition for our subsequent analysis of the relationship between B_0 and B_{hf}, to be discussed. However, we find larger variations for B_{hf} in the Alq_3 cation and NPB and TPD anions (1.39 mT, 0.65 mT, and 0.61 mT, respectively).

Regarding the different contributions to B_{hf}, we find surprising and unexpected results. As we mentioned, it is a common statement in the literature that hyperfine interactions in OMAR devices are due to hydrogen nuclei.[2,5,6,10,17,18] Our results show that this is not true in many cases: for TPD and NPB cations, the main contribution comes from the nitrogen nuclei, with just a modest contribution from hydrogen. The situation changes for TPD and NPB anions, for which the main contributors are indeed the hydrogen nuclei. For Alq_3 the main contribution is due to hydrogen, but with significant participation of aluminium for cations and nitrogen for anions. These different contributions from chemical species to B_{hf} come from the combined effects of the spatial distribution of the electronic spin density $n_s(\mathbf{r})$ (see Fig. 2) and the natural abundance of the isotope with nonzero nuclear spin (see Table I). As an example, let us analyze in detail the case of NPB. Our calculations shows an expressive spin density

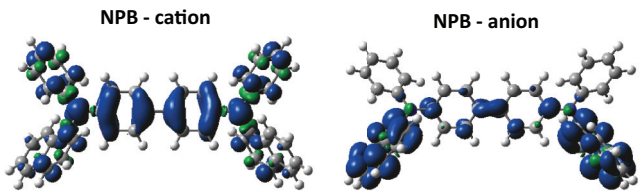

FIG. 2. (Color online) Density of spin $[n_s(\mathbf{r}) = n_\uparrow(\mathbf{r}) - n_\downarrow(\mathbf{r})]$ for NPB molecule. Isosurface value of 0.001 a.u. (atomic units).

around the nitrogen atoms for cations, which becomes small for anions (see Fig. 2). That explains why only for cations there is a significant contribution of nitrogen to B_{hf}. Our results also suggest that extra care is needed when analyzing the effects of deuteration in OMAR.[9,11]

Another interesting conclusion from our calculations is on the importance of the dipolar term (B_{dip}) to B_{hf}. It is a common approximation to model the hyperfine effects using only the Fermi contact term.[2,17,30] Our results show that this may not be a good approximation in some cases. For instance, in TPD and NPB cations, the contribution of the dipolar term is almost 50%. Our results also show that intramolecular dipolar contributions are much more important than extramolecular ones.

The relationship between B_0 and B_{hf} and HTL effects. As we mentioned, the typical OMAR field B_0 depends on several device parameters such as thickness or organic layers, bias voltage, temperature, and the particular choice of organic materials. A successful model relating B_0 and B_{hf} should be able to capture these dependences. This is a task beyond the scope of the present work. However, we address the particular issue of dependence on the choice of HTL. We do that by performing a direct comparison between our theoretically calculated B_{hf} and carefully controlled measurements of B_0 in two different HTL materials. To perform the measurements, it is desirable that our device has an approximately homogeneous B_{hf} across the organic layers. Therefore, guided by the theoretical findings displayed in Table II, we choose to work in encapsulated two-layer heterojunctions consisting of either 250 Å of NPB or TPD as hole-transport material and 500 Å of Alq_3 as electron-transport material, since all these molecules show $B_{hf} = 1.3$–1.4 mT for the appropriate charge carriers. So, it is expected that both devices show the same value of B_0. All the organic materials were thermally deposited in high vacuum environment onto patterned indium tin oxide glass substrates (1500 Å layer thickness) and a LiF:Al layer was used as cathode. The OMAR effect is measured using the magnetic field modulation technique[31] at room temperature.

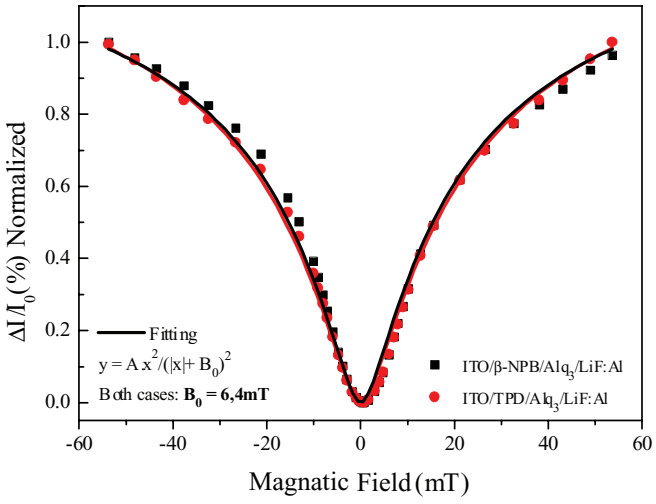

FIG. 3. (Color online) Magnetoresistance curves, at room temperature, of two encapsulated devices using β-NPB and TPD as hole transporting layer. In both cases, the measured characteristic field B_0 is 6.4 mT.

The system is able to detect OMAR signals from nanoampere to milliampere. Measurements are performed at a 10 V bias, which corresponds to current densities of about 95–100 A/m^2 for both NPB/Alq_3 and TPD/Alq_3 devices.

The resulting magnetoresistance curves are shown in Fig. 3. A key test for the rationale above is to find the same value of B_0 for the two devices. Indeed, data fit by a non-Lorentzian $\Delta I(B)/I \propto B^2/(|B| + B_0)^2$ curve gives amazingly $B_0 = 6.4$ mT for both devices. This value is roughly five times larger than our calculated B_{hf}, so our proportionality factor is $\alpha = 5$ for the specific conditions of our devices.

In conclusion, we designed and implemented a protocol for determining the average molecular hyperfine field B_{hf} of organic molecules used in OMAR devices that allows for quantitative and accurate theoretical determinations of B_{hf} that can be used as benchmarks to test existing models. Our calculations, based on *ab initio* methods, provided accurate results for such fields of selected molecular ions. We then constructed OMAR devices using molecular anions and cations with similar values of B_{hf}, ensuring that B_{hf} is homogeneous across the device. Then, measurements of the characteristic OMAR field B_0 probe the HTL dependence of such a quantity and allow for a direct comparison between this field and B_{hf}. As expected, molecules with the same value of B_{hf} produce the same B_0. In addition, contrary to common assumptions in the literature, we find that contributions to the molecular hyperfine fields are not restricted to hydrogen nuclei and dipolar terms can be as important as Fermi contact terms. Moreover, intramolecular contributions to the dipolar field are much more important than extramolecular ones.

We acknowledge financial support from Brazilian agencies CNPq, FAPERJ, Finep, and INEO-MCT for financial support.

*Author to whom correspondence should be addressed: rgiro@br.ibm.com—currently he is working at IBM Research Brazil.

[1] T. L. Francis, Ö. Mermer, G. Veeraraghavan, and M. Wohlgenannt, New J. Phys. **6**, 185 (2004).
[2] Y. Sheng, D. T. Nguyen, G. Veeraraghavan, Ö. Mermer, M. Wohlgenannt, S. Qiu, and U. Scherf, Phys. Rev. B **74**, 045213 (2006).
[3] V. N. Prigodim, J. Bergeson, D. M. Lincoln, and A. J. Epstein, Synth. Met. **156**, 757 (2006).
[4] J. L. Martin, J. D. Bergeson, V. N. Prigodin, and A. J. Epstein, Synth. Met. **160**, 291 (2010).
[5] P. A. Bobbert, T. D. Nguyen, F. W. A. van Oost, B. Koopmans, and M. Wohlgenannt, Phys. Rev. Lett. **99**, 216801 (2007).
[6] W. Wagemans, F. L. Bloom, and P. A. Bobbert, J. Appl. Phys. **103**, 07F303 (2008).
[7] B. Hu and Y. Wu, Nat. Mater. **6**, 985 (2007).
[8] N. J. Rolfe, M. Heeney, P. B. Wyatt, A. J. Drew, T. Kreouzis, and W. P. Gillin, Synth. Met. **161**, 608 (2011).
[9] T. D. Nguyen, G. Hukic-Markosian, F. Wang, L. Wojcik, X.-G. Li, E. Ehrenfreud, and Z. V. Vardeny, Nat. Mater. **9**, 345 (2010).
[10] P. A. Bobbert, W. Wagemans, F. W. A. van Oost, B. Koopmans, and M. Wohlgenannt, Phys. Rev. Lett. **102**, 156604 (2009).
[11] N. J. Rolfe, M. Heeney, P. B. Wyatt, A. J. Drew, T. Kreouzis, and W. P. Gillin, Phys. Rev. B **80**, 241201 (2009).
[12] J. Kalinowski, M. Cocchi, D. Virgili, P. Di Marco, and V. Fattori, Chem. Phys. Lett. **380**, 710 (2003).
[13] P. E. Blöchl, Phys. Rev. B **62**, 6158 (2000).
[14] K. J. R. Rosman and P. D. P. Taylor, Pure Appl. Chem. **70**, 217 (1998).
[15] I. Mills, T. Cvitas, K. Homann, N. Kallay, and K. Kuchits, *Quantities, Units and Symbols in Physical Chemistry* (Blackwell Scientific Publications, Oxford, UK, 1988).
[16] WebElements: http://www.webelements.com.
[17] K. Schulten and P. G. Wolynes, J. Chem. Phys. **68**, 3292 (1978).
[18] S. P. Kersten, A. J. Schellekens, B. Koopmans, and P. A. Bobbert, Phys. Rev. Lett. **106**, 197402 (2011).
[19] M. J. Frisch *et al.*, GAUSSIAN 03 Revision D.01, Gaussian, Inc., Wallingford, CT, 2004.
[20] J. P. Perdew, K. Burke, and M. Ernzerhof, Phys. Rev. Lett. **77**, 3865 (1996).
[21] J. P. Perdew, K. Burke, and M. Ernzerhof, Phys. Rev. Lett. **78**, 1396 (1997).
[22] C. Adamo and V. Barone, J. Chem. Phys. **110**, 6158 (1999).
[23] R. Ditchfield, W. J. Hehre, and J. A. Pople, J. Chem. Phys. **54**, 724 (1971).
[24] We also tested uncontracted basis sets for the calculation of hyperfine parameters. This option adds tight polarization functions to the core, which in principle should improve the accuracy of spin-spin coupling constants. However, tests for the Alq_3 molecule show that the use of uncontracted basis sets do not produce significant changes in the calculated values of B_{hf}.
[25] We hope that in a three-dimensional packed system, the charged geometry will be similar to neutral due to little space to accommodate the conformational change. Although all the geometries are optimized in vaccum, in your particular case, the charged (cation and anion) geometries are very similiar to neutron ones.
[26] Since only the dipolar term is present in extramolecular contributions and those nuclei are considerably more distant from the electron cloud than the intramolecular case, it is sufficient to consider that the spin density is given as a sum of Mulliken atomic charges to calculate the extramolecular terms.
[27] J.-A. Cheng and P.-J. Cheng, J. Chem. Crystallogr. **40**, 557 (2010).
[28] M. Brinkmann, G. Gadret, M. Muccini, C. Taliani, N. Masciocchi, and A. Sironi, J. Am. Chem. Soc. **122**, 5147 (2000).
[29] A. R. Kennedy, W. Ewen Smith, D. R. Tackley, W. I. F. David, K. Shankland, B. Brown, and S. J. Teat, J. Mater. Chem. **12**, 168 (2002).
[30] Y. Sheng, T. D. Nguyen, G. Veeraraghavan, Ö. Mermer, and M. Wohlgenannt, Phys. Rev. B **75**, 035202 (2007).
[31] H. Kahler and D. G. Seiler, Rev. Sci. Instrum. **48**, 1017 (1977).